Macromolecular Chemistry and Physic
www.mcp-journal.d

Scratch-Healing Surface-Attached Coatings from *Metallo*-Supramolecular Polymer Conetworks

Clément Mugemana, Anouk Martin, Patrick Grysan, Reiner Dieden, David Ruch, and Philippe Dubois*

Self-healing polymer coatings have gained increased attention as a pathway for regenerating the inherent properties of surface following mechanical, physical or chemical damages. In most cases, the adhesion between the polymer coating layer and the substrate is driven by physical interactions. For some applications, immersing the polymer coating under water or exposing the coating to organic solvent vapors will undoubtedly lead to the coating delamination. One way to circumvent this issue is to attach the coating to the substrate via covalent bonds. However, this process will impede the self-healing feature of the polymer coating due to the confinement of the volume change of the polymer to one dimension. Herein, surface-attached *metallo*-supramolecular polymer conetwork coatings are reported. The ability of the polymer conetworks to swell in organic solvent while maintaining their dimensional stability combined with reversible supramolecular cross-links based on metal complexes enables the design of scratch-healing polymer coatings. These *metallo*-supramolecular polymer conetworks are prepared in a three-step UV-initiated polymerization reaction starting from the poly(pentafluorophenyl acrylate)-*l*-polydimethylsiloxane (PPFPA-*l*-PDMS)-activated ester covalently attached to the substrate. Reacting the polymer conetwork coating with the 4-(2-aminoethyl)pyridine and cross-linking the pyridine phases with $ZnCl_2$ lead to the poly(*N*-(2(pyridin-4-yl)ethyl)acrylamide-Zn(II))-*l*-polydimethylsiloxane (PNP4EA-Zn(II)-*l*-PDMS) polymer conetwork coatings with scratch-healing ability.

1. Introduction

Self-healing coatings have attracted increasing attention as a promising alternative approach to extend the life span of functional surfaces by restoring their appearance and properties after damage for different applications including anticorrosion,[1] metal protective coating,[2] painting coating technology,[3] and others. Inspired by the work of White and co-workers in 2009,[4] extrinsic self-healing coatings based on microencapsulated healing agents that are released upon damage have been well-reported.[5] On the other hand, an intrinsic self-healing approach relies on the use of reversible bonds which can be covalent[6] such as Diels–Alder,[7,8] Schiff base,[9] thiol–ene chemistry,[10] and disulfide bonds.[11] Amongst a large variety of supramolecular interactions, hydrogen bonds based on a 2-ureido-4[1H]-pyrimidone linker were selected for the fabrication of self-healing polyurethane coatings.[12] Host–guest interactions from beta-cyclodextrin-modified silk fibroin (SCD) and adamantane-modified hyaluronic acid (HAD) evidenced the self-healing feature and antibacterial property.[13] Reversible supramolecular interactions based on metal complexes have mainly been explored for their self-healing property, because of the large numbers of ligands that can easily be introduced into polymers, and the fact that the strength of these interactions can simply be modulated by selecting the appropriate metal ions and the ligand.[14] Metal–ligand complexes based on terpyridine and Fe(II) were used to design self-healing coatings thanks to the reversible nature of these complexes.[15] Another interesting approach based on stimuli-responsive polyelectrolyte multilayers for the fabrication of self-healing coatings has been reported.[16] The polymer coatings were prepared using the layer-by-layer approach leading to mechanically robust coatings. The self-healing property was achieved by immersing the polymer coating in water, allowing the polymer chains flowability and to repair cuts that were several tens of micrometers deep and wide.[17] Nevertheless, immersing the coating for a prolonged period could cause substantial swelling and contraction, subsequently leading to the delamination of the coating from the substrate.

Amphiphilic polymer conetworks (APCNs) with covalently interconnected phase-separated domains represent an attractive class of polymeric materials.[18] Their ability to swell in both aqueous and organic media while maintaining their

Dr. C. Mugemana, A. Martin, P. Grysan, Dr. R. Dieden, Dr. D. Ruch
Luxembourg Institute of Science and Technology
Materials Research and Technology Department
5 rue Bommel – ZAE Robert Steichen, Hautcharage L-4940, Luxembourg
E-mail: clement.mugemana@list.lu
Prof. P. Dubois
Center of Innovation and Research in Materials Polymers
Laboratory of Polymeric and Composite Materials
Université de Mons
Place du Parc, Mons 23B-7000, Belgium
The ORCID identification number(s) for the author(s) of this article can be found under https://doi.org/10.1002/macp.202000331.

DOI: 10.1002/macp.202000331

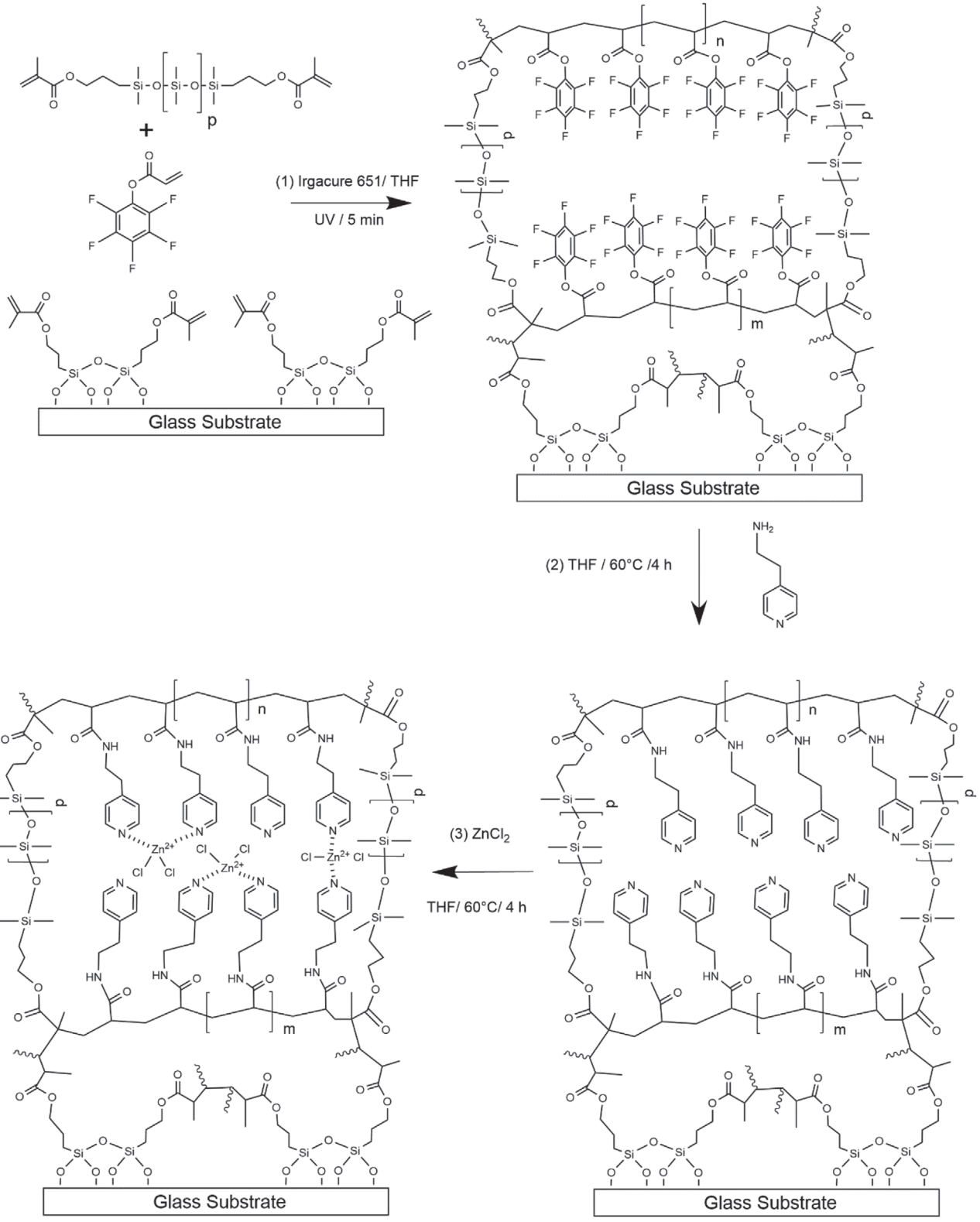

Figure 1. Three-step synthesis of *metallo*-supramolecular amphiphilic polymer conetwork coatings: simplified representations of 1) PPFPA-*l*-PDMS, 2) PNP4EA-*l*-PDMS, and 3) PNP4EA-Zn(II)-*l*-PDMS.

dimensional stability and without encountering macroscopic phase separation or polymer leaching remains one of the key features of APCNs.[19] The swelling ability of the APCNs has been exploited for the design of a self-sealing coating that has the ability to close punctures.[20] Nevertheless, the healing was not permanent, as the coating had to remain in a swollen state to reach an efficient sealing property. Recently, self-healing *metallo*-supramolecular polymer conetwork films were reported and the impact of the metal complexes on the recovery of mechanical properties after healing has been demonstrated.[21] Herein, the self-healing ability is optimized for surface-attached *metallo*-polymer conetwork coatings.

2. Results and Discussion

PFPA has been reported as a suitable hydrophobically masked monomer that is simultaneously in active ester and therefore allows us to prepare a wide range of functionalized poly(acrylamide)-based APCNs.[22] The PPFPA-*l*-PDMS conetwork precursor coatings were synthesized by UV-initiated polymerization in the presence of Irgacure 651 (2,2-dimethoxy-1,2-diphenylethan-1-one). To ensure a covalent bond between the polymer coating and the substrate, the glass substrates (2.6 × 3 cm^2) were reacted with 3-(trimethoxysilyl)propyl methacrylate to covalently attach methacrylate groups onto the surface according to the previously reported procedure.[18a] The polydimethylsiloxane dimethacrylate (PDMS-DMA) cross-linker was mixed with the PFPA monomer at a 1:1 weight ratio. The resulting monomer mixture was diluted with THF into which Irgacure 651 had been dissolved. (**Figure 1**) A 50 µm thick polypropylene tape was placed on the edges of the methacrylate functionalized-glass substrate to form a U-shape mould as depicted in Figure S2 of the Supporting Information. The polymer coating was prepared by a solution casting method, and a glass slide covered by a polypropylene tape was placed on top of the monomer mixture, which was directly photopolymerized under UV light for 2.5 min from each side. Unreacted monomers and PDMS cross-linkers were extracted by immersing the coatings in THF for 24 h at room temperature. An ATR-FTIR analysis of the APCNs coatings revealed the characteristic absorption bands of the active ester at 1783 cm^{-1} (C=O stretch) and the fluorinated aromatic ring stretch at 1520 cm^{-1}. (**Figure 2**) The surface analysis of the PPFPA-*l*-PDMS coatings by AFM height and phase analysis revealed nanophase morphologies typical of APCNs with larger interconnected PDMS spherical nanodomains of 26 ± 2 nm in diameter, dispersed in a PPFPA matrix (**Figure 3**a,b) compared to our previous study where smaller PDMS nanodomains of 10 nm in diameter were observed.[21]

The next step consisted of reacting the 4-(2-aminoethyl) pyridine with the activated ester to functionalize the pyridine ligand into the APCNs coating. The 4-(2-aminoethyl)pyridine was selected because of its higher reactivity in the presence of the activated esters and higher binding strength with metal ions compared to 4-aminopyridine.[23] To this end, the coating was immersed in THF containing 0.8 M of 4-(2-aminoethyl)pyridine and the reaction was carried out at 60 °C for 4 h (Figure 1). The functionalization of pyridine ligand was confirmed by an ATR-FTIR analysis. The PNP4EA-*l*-PDMS coatings evidenced the amide stretch signal peak at 1652 cm^{-1},

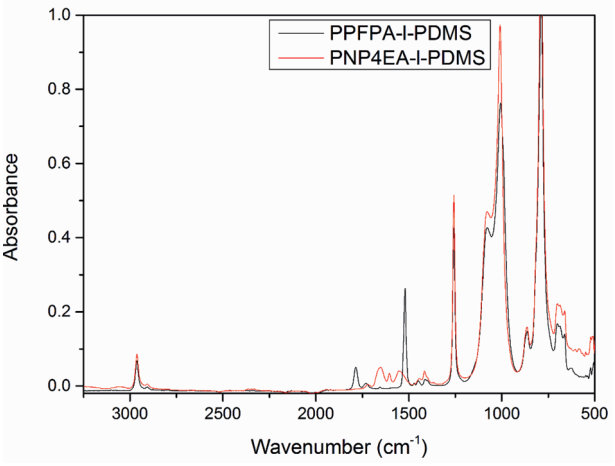

Figure 2. ATR-FTIR spectra of the PPFPA-*l*-PDMS (red) and PNP4EA-*l*-PDMS (black) polymer conetwork coatings.

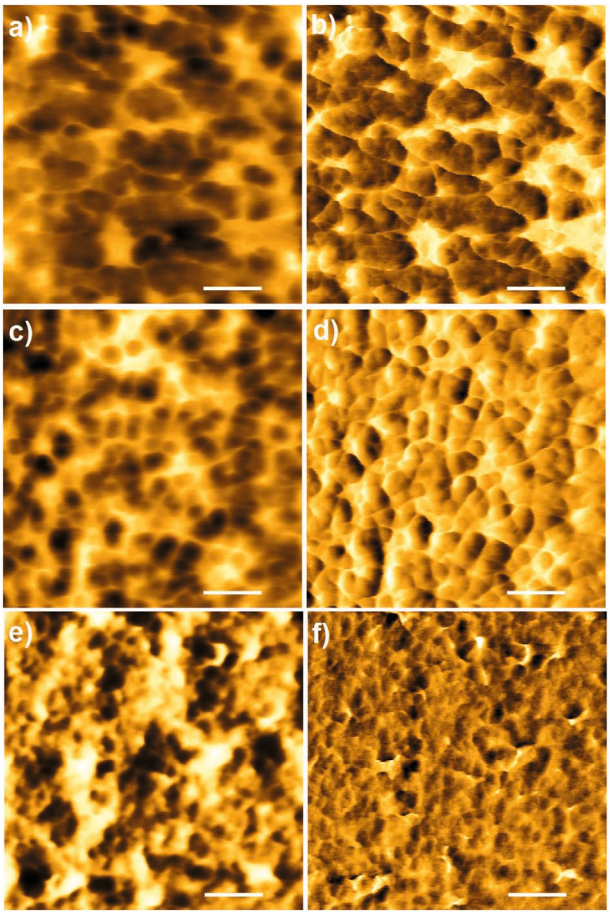

Figure 3. AFM height and phase mode images of PPFPA-*l*-PDMS (a) height and (b) phase); PNP4EA-*l*-PDMS (c) height and (d) phase and PNP4EA-Zn(II)-*l*-PDMS (e) height and (f) phase of the surface of the polymer conetworks coatings. Scale bar: 100 nm.

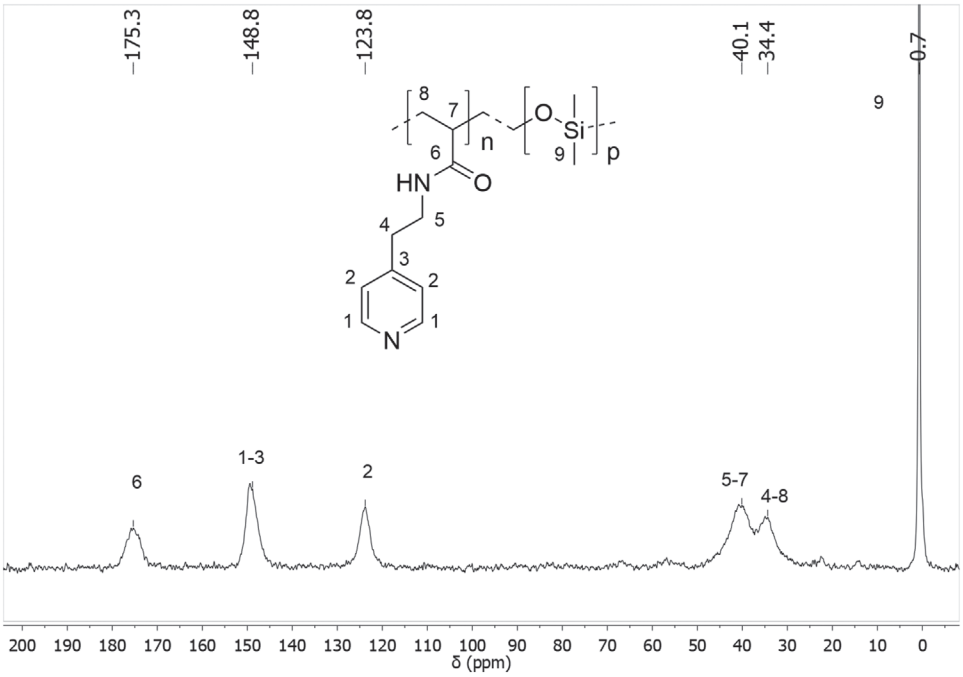

Figure 4. Solid-state ^{13}C NMR spectrum of the PNP4EA-*l*-PDMS polymer conetworks coating.

and the pyridine ring vibration signal shifted at 1606 cm^{-1} (Figure 2).

A solid-state ^{13}C NMR analysis of the PNP4EA-*l*-PDMS polymer conetworks revealed well-defined characteristic peaks of the carbonyl and pyridine ligand with chemical shifts respectively at 175 ppm CO(5), 148 ppm CH(1-3), and 123 ppm C(3) thus confirming the successful functionalization with the pyridine ligand (**Figure 4**). A solid-state ^{1}H NMR analysis in swollen state using $CDCl_3$ solvent complemented the ^{13}C NMR by revealing characteristic aromatic proton signals of the PNP4EA phases as depicted in Figure S7 of the Supporting Information. The surface analysis of the PNP4EA-*l*-PDMS obtained by the functionalization of the APCNs with the 4-(2-aminoethyl)pyridine did not reveal any change of the nanophase morphology neither the sizes of the PDMS domains (Figure 3c,d).

The following step consisted of loading $ZnCl_2$ into the polymer conetwork. As previously reported, $ZnCl_2$ complexes were selected to provide reversible interactions needed for the self-healing feature. Furthermore, Zn(II) ions can provide antibacterial[24] and anticorrosion properties[25] to the surface, thus enlarging the application of the designed *metallo*-polymer coatings. To this end, the coatings were immersed in THF solution containing $ZnCl_2$ (3.67×10^{-3} M), and the reaction was carried out at 60 °C for 4 h. The polymer coatings were then rinsed in THF and dried under vacuum. The loading of $ZnCl_2$ salt into the polymer conetwork coating led to the cross-linking of the PNP4EA phases via intra- and intermolecular cross-linking as depicted in Figure 1. It is hypothesized that intermolecular cross-linking would lead to the self-healing feature. The addition of the $ZnCl_2$ induced the shrinking of the PDMS phases by ≈10 nm as shown in Figure 3e,f and this behavior could be assigned to intermolecular cross-linking within the PNE4EA, which impacted the nanophase morphology. The complexation of Zn(II) ions by pyridine ligand was confirmed by ATR-FTIR analysis, which revealed a shift of the characteristic pyridine ring vibration signal from 1606 to 1620 cm^{-1} (Figure S6, Supporting Information).

The concentration of the Zn(II) ions of 8.5 ± 0.1 wt% was determined by inductively coupled plasma mass spectrometry analysis and corresponded to a molar ratio of PNP4EA to Zn(II) close to 2:1, which is similar to that reported for the *metallo*-polymer conetwork films.[21] The cross-section of the polymer coating was measured by optical microscope and revealed that loading of Zn(II) resulted in an increase of the thickness from 34.5 ± 1.6 µm (PNP4EA-*l*-PDMS) to 47 ± 1 µm (PNP4EA-Zn(II)-*l*-PDMS) as a result of the complexation of Zn(II) ions by the PNP4EA phases (Figure S5, Supporting Information).

One of the attractive features of the amphiphilic polymer conetwork coating is its ability to swell in both aqueous and organic media while preserving its dimensional stability and without encountering macroscopic phase separation. The polymer conetwork films of the same composition and based on the PNP4EA-*l*-PDMS and PNP4EA-Zn(II)-*l*-PDMS polymer conetworks were prepared following the previously described procedure.[21] Their equilibrium volumetric degrees of swelling were tested in organic solvents: THF, 2-propanol and n-hexane. In THF and 2-propanol, the PNP4EA-*l*-PDMS polymer conetworks films showed a fast swelling in 2 h and the equilibrium swelling degree was reached in 5 h (**Figure 5**a). In n-hexane, a selective solvent of the PDMS phases the equilibrium swelling degree was reached faster in half an hour, with a volumetric swelling degree of ≈2.5 in 24 h. The average swelling volumetric degree of 4.8 ± 0.2 and 4.4 ± 0.4 were measured after 24 h in THF and 2-propanol, respectively (Figure 5c). The cross-linking of the PNP4EA phases by Zn(II) ions reduced the overall

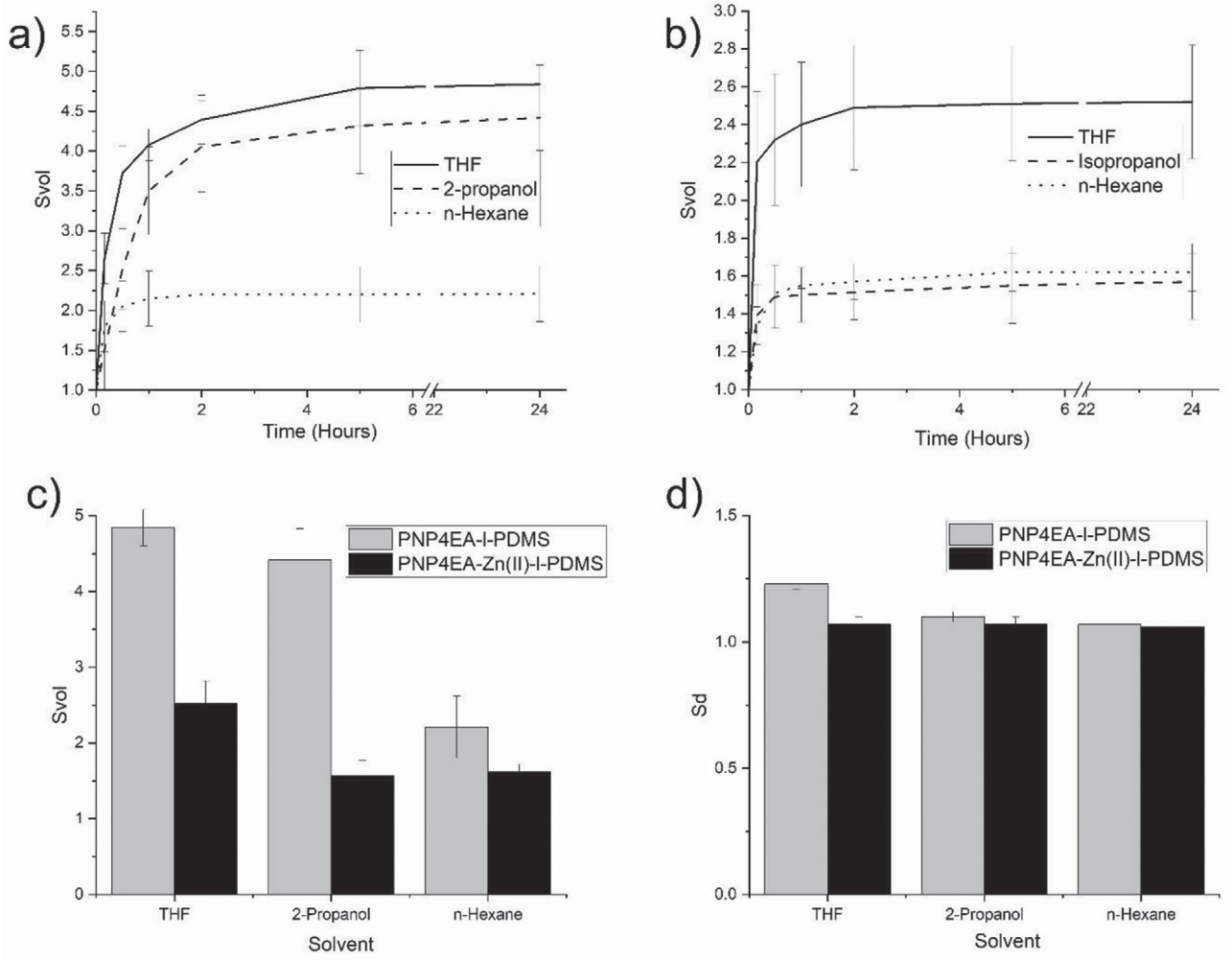

Figure 5. The volumetric degree of swelling S_{Vol} versus time of swelling for a) the PNP4EA-*l*-PDMS and b) PNP4EA-Zn(II)-*l*-PDMS b) polymer conetworks films in organic solvents; c) the volumetric degree of swelling in 24 h and d) 1D swelling degree of (Sd) of the polymer conetwork coatings in organic solvents. (Mean values of $n = 3$ independent measurements, error bars represent SD.)

swelling ability. The highest swelling degree was achieved in THF, with an equilibrium swelling degree of ≈2.5, while in 2-propanol and n-hexane, a swelling volumetric degree of 1.6 was measured within 2 h. It is noteworthy to mention that the overall swelling degree remained constant up to 24 h, which proved that the bound metal ions are not released in organic solvent. It has been previously demonstrated that a polymer conetwork covalently attached to a surface results in the confinement of the volume change to one dimension, normal to the surface, which substantially reduces the swelling beh avior.[18a],[26] This was proved by measuring the 1D swelling of the polymer coating cross-section. In THF, the swelling degree corresponding to 1.25 was measured, while in 2-propanol and n-hexane only 1.10 and 1.07 were measured, respectively. The measured values are close to the equilibrium swelling degree of the PHEA-*l*-PDMS polymer conetwork coating corresponding to ≈1.10 with similar ratio (PHEA:PDMS 1:1) in n-hexane and water.[18a] This confirmed the impact of the surface attachment by reducing the swelling ability of the polymer conetworks. The loading of $ZnCl_2$ into the polymer conetworks reduced further the swelling degree of the polymer coatings at room temperature with an equilibrium swelling degree of ≈1.07 for the tested organic solvents (Figure 5d).

The mechanical properties of the prepared polymer conetworks films were assessed by tensile tests analysis. The PNP4EA-*l*-PDMS polymer conetworks exhibited a tensile strength of 5.2 ± 0.6 MPa and a Young modulus (E') of ≈2.1 ± 0.3 MPa with a strain at break of 41 ± 5 at a strain rate of 10 mm min^{-1}. Loading the metal complex into the polymer conetwork reduced the strain break to 1.2 ± 0.3 due to the crosslinking of the PN4EA phases, but on the other hand these interactions increased the Young's modulus (E') up to 6.7 ± 0.5 MPa, with a tensile strength corresponding to 7.4 ± 0.7 MPa (**Figure 6**).

The healing ability of the polymer conetworks was tested by scratching the surface of the coating using a scalpel, resulting in a 15 µm wide scratch. Preliminary scratch-healing tests were carried out in the conditions previously used for the polymer conetworks films.[21] In this case, no healing of the scratch was observed as the coating was covalently attached to the substrate. Therefore, despite the poor swelling ability of the polymer

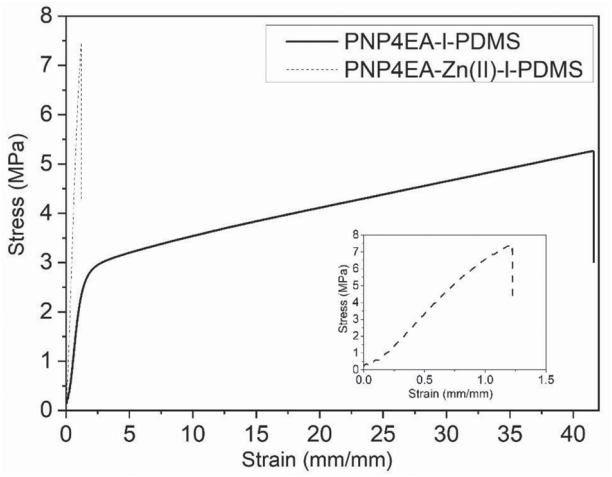

Figure 6. Uniaxial tensile tests of the PNP4EA-*l*-PDMS polymer conetworks (solid line) and the polymer conetworks PNPE4A-Zn(II)-*l*-PDMS loaded with $ZnCl_2$ (dashed line) at a strain rate of 10 mm min^{-1}.

coating in organic solvents at room temperature, the scratch-healing ability was tested in the presence of the organic solvent. It was hypothesized that upon heating, the swelling ability would increase, thus mediating the healing process. To this end, THF was dropped on the scratched area (**Figure 7**a) and the coating was placed in an oven heated at 65 °C for 2 h. In this condition, optical microscope images evidenced the healing of the scratch, confirming the hypothesis of the solvent evaporation-mediated healing (Figure 7b). A similar test was performed in the presence of 2-propanol and the damaged coating was heated at 80 °C (the boiling point of 2-propanol: 82.5 °C) for 2 h. In this case, the healing of the scratch was observed leaving a scar, as shown in Figure 7d. To prove that the healing effect is controlled by the swelling of the PNP4EA-Zn(II) phases, the scratch healing was tested in the presence of n-hexane, a selective solvent of the PDMS phase, for 2 h at 65 °C (Figure 7e).

However, in the presence of n-hexane, the scratch was still observed on the surface as a result of the collapse of the PNP4EA-Zn(II) phases. (Figure 7f) To demonstrate the impact

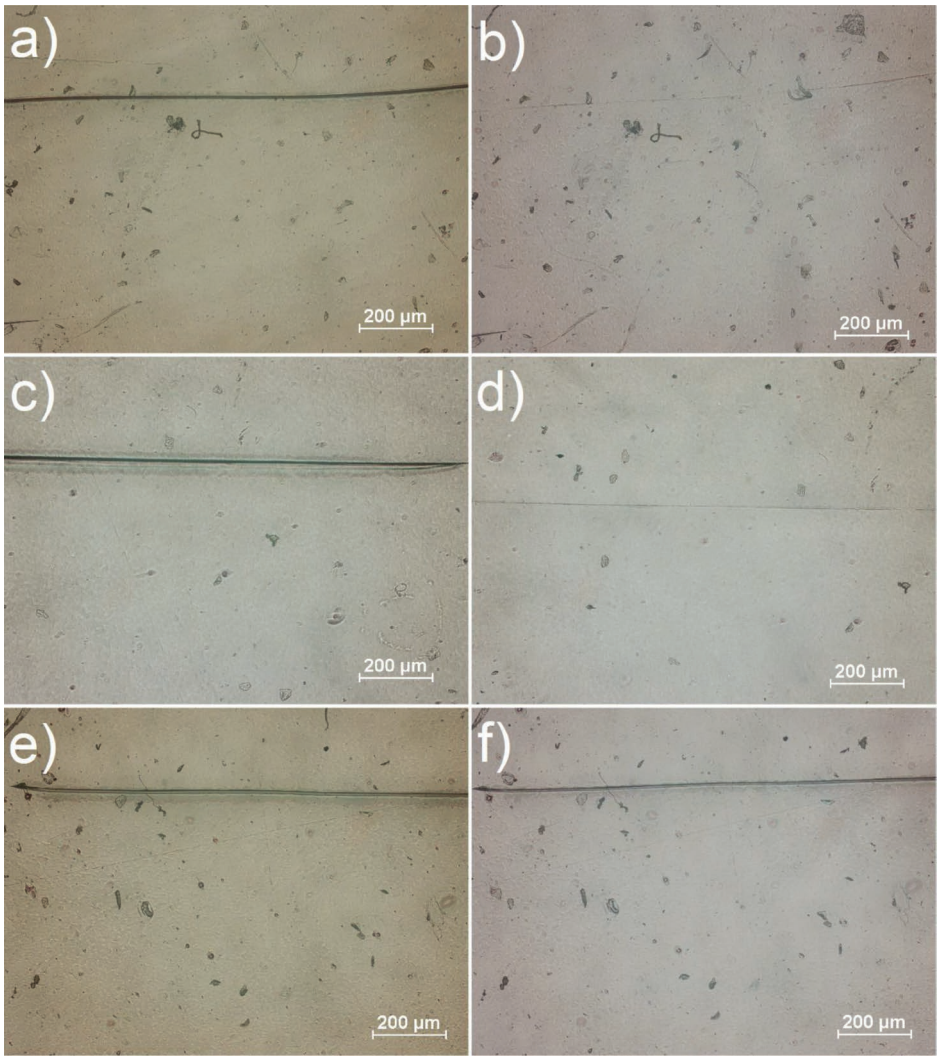

Figure 7. Optical microscope images of the scratched surface-attached coatings from the PNP4EA-Zn(II)-l-PDMS polymer conetworks (a,c,e) and after healing in the presence of b) THF, d) 2-propanol, and f) n-hexane.

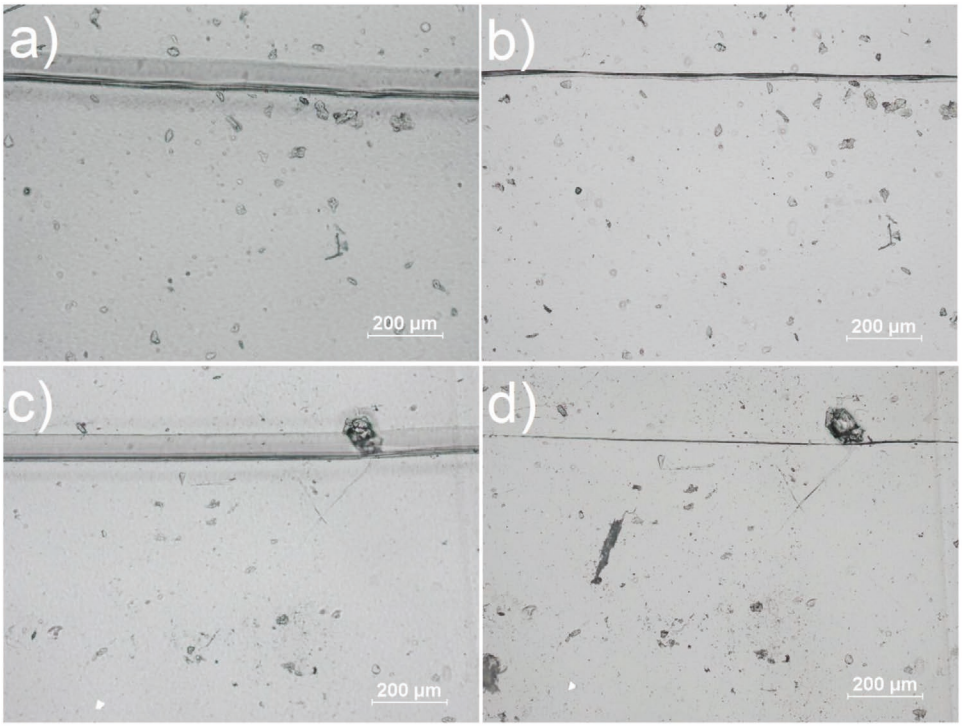

Figure 8. Optical microscope images of the scratched polymer coatings from the PNP4EA-*l*-PDMS polymer conetworks (a and c) and following the exposure to THF (b) and 2-propanol (d) solvents.

of the reversible bond Zn(II)–pyridine complexes on the self-healing feature, a scratch was made on Zn(II)-free polymer coatings (PNP4EA-*l*-PDMS). The same healing conditions were applied by dropping THF and 2-propanol on the scratched area separately (**Figure 8**a,c). Despite the measured higher swelling ability of the coating in THF (Figure 5d), no healing was observed for THF and 2-propanol (Figure 8b,d), thus confirming the essential role of the reversible bonds to achieve permanent healing on the surface of the coatings.

In conclusion, surface-attached coatings based on PNP4EA-Zn(II)-*l*-PDMS *metallo*-polymer conetworks were synthesized, and the corresponding phase-separated nanostructured morphologies were evidenced by AFM analysis while their composition was confirmed by the solid-state ^{13}C NMR analysis. The swelling ability of the APCNs films and coatings was investigated, as well as the impact of the reversible cross-links by the Zn(II)–pyridine complexes. The scratch-healing ability mediated by organic solvent evaporation was demonstrated on the surface-attached polymer coatings. The reversible cross-link supramolecular interactions based on pyridine–Zn(II) complexes enabled permanent scratch-healing. The synthesized *metallo*-supramolecular polymer conetwork coatings could find application for underwater coatings and the complexed Zn(II) ions enlarges their field of application to antibacterial surfaces.

Supporting Information

Supporting Information is available from the Wiley Online Library or from the author.

Acknowledgements

The authors thank the FNR (Luxembourg National Research Fund) for its financial support for the SUSMAT project through the PEARL programme.

Conflict of Interest

The authors declare no conflict of interest.

Keywords

activated esters, amphiphilic polymer conetworks (APCNs), *metallo*-supramolecular polymers, self-healing, surface-attached coatings, zinc(II) complexes

Received: September 30, 2020
Revised: December 2, 2020
Published online:

[1] a) A. Stankiewicz, I. Szczygieł, B. Szczygieł, *J. Mater. Sci.* **2013**, *48*, 8041; b) F. Zhang, P. Ju, M. Pan, D. Zhang, Y. Huang, G. Li, X. Li, *Corros. Sci.* **2018**, *144*, 74; c) A. Lutz, O. van den Berg, J. Wielant, I. De Graeve, H. Terryn, *Front. Mater.* **2016**, *2*, 112
[2] D. G. Shchukin, *Polym. Chem.* **2013**, *4*, 4871.
[3] E. Koh, N.-K. Kim, J. Shin, Y.-W. Kim, *RSC Adv.* **2014**, *4*, 16214.
[4] S. H. Cho, S. R. White, P. V. Braun, *Adv. Mater.* **2009**, *21*, 645.
[5] a) M. Samadzadeh, S. H. Boura, M. Peikari, S. M. Kasiriha, A. Ashrafi, *Prog. Org. Coat.* **2010**, *68*, 159; b) C. Suryanarayana, K. C. Rao, D. Kumar, *Prog. Org. Coat.* **2008**, *63*, 72.

[6] J. Dahlke, S. Zechel, M. D. Hager, U. S. Schubert, *Adv. Mater. Interfaces* **2018**, *5*, 1800051.
[7] C. D. Roland, T. S. Kleine, J. A. Orlicki, P. J. Costanzo, *Polym. Prepr. (Am. Chem. Soc., Div. Polym. Chem.)* **2012**, *53*, 717.
[8] a) J. Liu, Z. Zhou, X. Su, J. Cao, M. Chen, R. Liu, *Prog. Org. Coat.* **2020**, *146*, 105699; b) Z. Wang, H. Yang, B. D. Fairbanks, H. Liang, J. Ke, C. Zhu, *Prog. Org. Coat.* **2019**, *131*, 131; c) D. H. Turkenburg, Y. Durant, H. R. Fischer, *Prog. Org. Coat.* **2017**, *111*, 38; d) J. Kötteritzsch, S. Stumpf, S. Hoeppener, J. Vitz, M. D. Hager, U. S. Schubert, *Macromol. Chem. Phys.* **2013**, *214*, 1636.
[9] J. Ren, M. Li, R. Yuan, A. Pang, Z. Lu, L. Ge, *Colloids Surf. A* **2020**, *586*, 124203.
[10] Z. Wang, H. Liang, H. Yang, L. Xiong, J. Zhou, S. Huang, C. Zhao, J. Zhong, X. Fan, *Prog. Org. Coat.* **2019**, *137*, 105282.
[11] D. Zhao, S. Liu, Y. Wu, T. Guan, N. Sun, B. Ren, *Prog. Org. Coat.* **2019**, *133*, 289.
[12] F. Gao, J. Cao, Q. Wang, R. Liu, S. Zhang, J. Liu, X. Liu, *Prog. Org. Coat.* **2017**, *113*, 160.
[13] H. Xuan, X. Tang, Y. Zhu, J. Ling, Y. Yang, *ACS Appl. Bio Mater.* **2020**, *3*, 1628.
[14] a) C. Mugemana, P. Guillet, S. Hoeppener, U. S. Schubert, C.-A. Fustin, J.-F. Gohy, *Chem. Commun.* **2010**, *46*, 1296;. b) X. Xu, F. A. Jerca, V. V. Jerca, R. Hoogenboom, *Adv. Funct. Mater.* **2019**, *29*, 1904886; c) C. Mugemana, J.-F. Gohy, C.-A. Fustin, *Langmuir* **2012**, *28*, 3018;. d) P. Guillet, C. Mugemana, F. J. Stadler, U. S. Schubert, C.-A. Fustin, C. Bailly, J.-F. Gohy, *Soft Matter* **2009**, *5*, 3409.
[15] S. Bode, L. Zedler, F. H. Schacher, B. Dietzek, M. Schmitt, J. Popp, M. D. Hager, U. S. Schubert, *Adv. Mater.* **2013**, *25*, 1634.
[16] N. Y. Abu-Thabit, A. S. Hamdy, *Surf. Coat. Technol.* **2016**, *303*, 406.
[17] X. Wang, F. Liu, X. Zheng, J. Sun, *Angew. Chem., Int. Ed.* **2011**, *50*, 11378.
[18] a) N. Bruns, J. Scherble, L. Hartmann, R. Thomann, B. Iván, R. Mülhaupt, J. C. Tiller, *Macromolecules* **2005**, *38*, 2431; b) C. S. Patrickios, *Amphiphilic Polymer Co-networks: Synthesis, Properties, Modelling and Applications*, The Royal Society of Chemistry, London **2020**, pp. 1–14.
[19] a) G. Erdodi, J. P. Kennedy, *Prog. Polym. Sci.* **2006**, *31*, 118; b) T. Stumphauser, G. Kasza, A. Domján, A. Wacha, Z. Varga, Y. Thomann, R. Thomann, B. Pásztói, T. M. Trötschler, B. Kerscher, R. Mülhaupt, B. Iván, *Polymers* **2020**, *12*, 2292.
[20] M. Rother, J. Barmettler, A. Reichmuth, J. V. Araujo, C. Rytka, O. Glaied, U. Pieles, N. Bruns, *Adv. Mater.* **2015**, *27*, 6620.
[21] C. Mugemana, P. Grysan, R. Dieden, D. Ruch, N. Bruns, P. Dubois, *Macromol. Chem. Phys.* **2020**, *221*, 1900432.
[22] S. Ulrich, A. Sadeghpour, R. M. Rossi, N. Bruns, L. F. Boesel, *Macromolecules* **2018**, *51*, 5267.
[23] A. Das, P. Theato, *Chem. Rev.* **2016**, *116*, 1434.
[24] a) Y. Yonehara, H. Yamashita, C. Kawamura, K. Itoh, *Prog. Org. Coat.* **2001**, *42*, 150; b) Y. Feng, S. Chen, Y. Frank Cheng, *Surf. Coat. Technol.* **2018**, *340*, 55.
[25] a) X. Shi, T. A. Nguyen, Z. Suo, Y. Liu, R. Avci, *Surf. Coat. Technol.* **2009**, *204*, 237; b) L. Zhang, A. Ma, J. Jiang, D. Song, J. Chen, D. Yang, *Prog. Nat. Sci.: Mater. Int.* **2012**, *22*, 326.
[26] R. Toomey, D. Freidank, J. Rühe, *Macromolecules* **2004**, *37*, 882.